Materials Science-Poland, Vol. 24, No. 1, 2006

$La_{1-x}Sr_xCo_{1-y-z}Fe_yNi_zO_3$ perovskites – possible new cathode materials for intermediate-temperature solid-oxide fuel cells

K. ŚWIERCZEK*, J. MARZEC, J. MOLENDA

Faculty of Materials Science and Ceramics, AGH University of Science and Technology,
al. Mickiewicza 30, 30-059 Cracow, Poland

$La_{1-x}Sr_xCo_{1-y-z}Fe_yNi_zO_3$ perovskites have been synthesized with hexagonal *R*-3*c* structures by a modified citric acid method and determined their structural and transport properties. Structural instabilities for samples with high Ni and Sr content heated to 1270 K were observed, leading to the appearance of secondary phases with spinel structures. Moessbauer studies revealed the presence of two different, clearly distinguishable surroundings of Fe ions, despite single crystallographic positions of iron ions. Low-temperature (77–300 K) dc conductivity and thermoelectric power measurements suggest an activated charge transport mechanism with the activation energy strongly dependent on the chemical composition of the material. Electrical conductivity as a function of temperature suggests the appearance of a hopping mechanism. The observed high-temperature (870–1070 K) dc electrical conductivity of $La_{1-x}Sr_xCo_{1-y-z}Fe_yNi_zO_3$ samples is relatively high and strongly depends on chemical composition. It seems possible to optimise the transport properties of $La_{1-x}Sr_xCo_{1-y-z}Fe_yNi_zO_3$ by chemical composition, which may lead to a new, attractive cathode material in terms of possible applications in intermediate -temperature solid-oxide fuel cells (IT-SOFCs).

Key words: *perovskite; solid-oxide fuel cell; cathode material; transport properties*

1. Introduction

Lowering the working temperature of high-temperature solid-oxide fuel cells (to the 600–800 ºC range) seems to be very important with respect to further developing the SOFC technology. Beneficial results will be a decrease in high-temperature corrosion and chemical degradation, usage of cheaper and more environmentally friendly materials for cell stack construction, as well as reduction of problems with cell stack

*Corresponding author, e-mail: xi@uci.agh.edu.pl

sealing. State of the art materials used in high temperature SOFCs, however, do not perform well in the intermediate temperature region.

New materials, which can replace currently used ZrO_2-based electrolytes and $La_{1-x}Sr_xMnO_{3\pm\delta}$ or other manganese-based perovskite cathodes, have been studied. Among the possible candidates for the cathode material, Co and Fe-based perovskites seem interesting due to their high catalytic activities and electrical conductivities [1, 2]. Ni-based perovskites have also been studied due to the high, metallic-like conductivity of $LaNiO_3$; these, however, suffer from lower thermal stability [3]. Perovskites with mixed composition, i.e. $La_{1-x}Sr_xCo_{1-y}Fe_yO_3$, exhibit even better properties in terms of their possible applications [4, 5].

The aim of this study was to investigate materials from a La–Sr–Co–Fe–Ni perovskite system in terms of their possible applications as cathodes for IT-SOFCs.

2. Experimental

$La_{1-x}Sr_xCo_{1-y-z}Fe_yNi_zO_3$ perovskites were synthesized using precursors obtained by the modified citric acid method; details of the synthesis procedure can be found elsewhere [6]. Final heating was conducted at 1270 K in air for 24 h with an initial step at 1070 K for 12 h. The obtained samples were characterized by XRD studies (Phillips X'Pert Pro). The X-ray spectra were analysed using the Rietveld method. For $La_{1-x}Sr_xCo_{0.4}Fe_{0.4}Ni_{0.2}O_3$ samples, the local structure of iron ions was characterized by ^{57}Fe Moessbauer spectroscopy. Scanning electron microscopy, together with EDS spectroscopy, was performed on perovskite powders. dc electrical conductivity was measured by a pseudo 4-probe method, and electrodes were made using silver paint. Thermoelectric power was calculated from the slope of the dependence of thermoelectric voltage on the variable temperature gradient ($\Delta T \approx 0$–3K).

3. Results

The results of X-ray measurements performed for various $La_{1-x}Sr_xCo_{1-y-z}Fe_yNi_zO_3$ perovskites obtained by the citric acid route are presented in Table 1. We were able to obtain single phase $La_{1-x}Sr_xCo_{1-y-z}Fe_yNi_zO_3$ perovskites with small amounts of Sr and Ni. For all samples with $x + z > 0.6$, secondary phases appear. The observed secondary phases possess spinel structures and most likely have a La_2NiO_4-like composition for materials with higher Ni content or a Sr_2FeO_4-like composition for materials with higher Sr content. For some two-phase samples, a lowering of the final heating temperature from 1270 K to 1070 K leads to a single-phase system. This temperature is too low, however, in terms of possible application in the IT-SOFCs. X-ray results suggest that the La–Sr–Co–Fe–Ni system is complicated and that the allowed solid solution range is relatively small. It is worth noting that in La_2NiO_4 the valence of

nickel ions is 2+. This suggests that the $La_{1-x}Sr_xCo_{1-y-z}Fe_yNi_zO_3$ instability for $x + z > 0.6–0.7$ is strongly linked to the valence of 3d metals.

Table 1. Structural properties of $La_{1-x}Sr_xCo_{1-y-z}Fe_yNi_zO_3$ perovskites

Composition	Structure	*a* [Å]	*c* [Å]	Cell volume [Å]^3
$La_{0.9}Sr_{0.1}Co_{0.2}Fe_{0.6}Ni_{0.2}O_3$	*R*-3*c*	5.5097(2)	13.3101(7)	349.92(3)
$La_{0.8}Sr_{0.2}Co_{0.2}Fe_{0.6}Ni_{0.2}O_3$	*R*-3*c*	5.4963(2)	13.3179(6)	348.42(2)
$La_{0.7}Sr_{0.3}Co_{0.2}Fe_{0.6}Ni_{0.2}O_3$	*R*-3*c*	5.4814(2)	13.3180(7)	346.54(3)
$La_{0.6}Sr_{0.4}Co_{0.2}Fe_{0.6}Ni_{0.2}O_3$	two phase	–	–	–
$La_{0.9}Sr_{0.1}Co_{0.4}Fe_{0.4}Ni_{0.2}O_{3-\delta}$	*R*-3*c*	5.4818(2)	13.2423(5)	344.62(2)
$La_{0.8}Sr_{0.2}Co_{0.4}Fe_{0.4}Ni_{0.2}O_{3-\delta}$	*R*-3*c*	5.4745(2)	13.2584(5)	344.12(2)
$La_{0.7}Sr_{0.3}Co_{0.4}Fe_{0.4}Ni_{0.2}O_{3-\delta}$	*R*-3*c*	5.4620(2)	13.2732(7)	342.93(3)
$La_{0.9}Sr_{0.1}Co_{0.2}Fe_{0.4}Ni_{0.4}O_{3-\delta}$	*R*-3*c*	5.4866(2)	13.2576(5)	345.62(2)
$La_{0.8}Sr_{0.2}Co_{0.2}Fe_{0.4}Ni_{0.4}O_{3-\delta}$	*R*-3*c*, traces of spinel phase	5.4769(2)	13.2764(6)	344.89(2)
$La_{0.9}Sr_{0.1}Co_{0.5}Fe_{0.4}Ni_{0.1}O_3$	*R*-3*c*	5.4777(2)	13.2335(5)	343.88(2)
$La_{0.8}Sr_{0.2}Co_{0.5}Fe_{0.4}Ni_{0.1}O_3$	*R*-3*c*, traces of spinel phase	5.4709(3)	13.2578(7)	343.65(3)

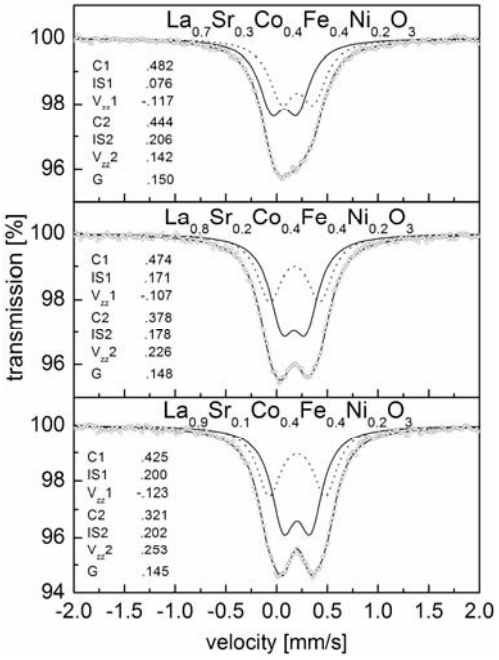

Fig. 1. Moessbauer spectra of $La_{1-x}Sr_xCo_{0.4}Fe_{0.4}Ni_{0.2}O_3$ perovskites

Moessbauer studies for $La_{1-x}Sr_xCo_{0.4}Fe_{0.4}Ni_{0.2}O_3$ samples (Fig. 1) revealed the presence of two different, clearly distinguishable surroundings of Fe ions, despite

a single crystallographic position of iron ions (6b). A comparison of these results with previous studies for $La_{1-x}Sr_xCo_{0.2}Fe_{0.6}Ni_{0.2}O_3$ compositions [6] leads to the conclusion that this differentiation is driven by the La–Sr sublattice. The first coordination sphere of Fe in the *R*-3*c* perovskite structure is the FeO_6 octahedron, the second coordination sphere is cube-shaped, with Fe in the centre and La and Sr ions randomly occupying the corners. It seems that the observed Moessbauer spectra may originate from a superstructure formed by the possible ordering of La and Sr ions within this sublattice.

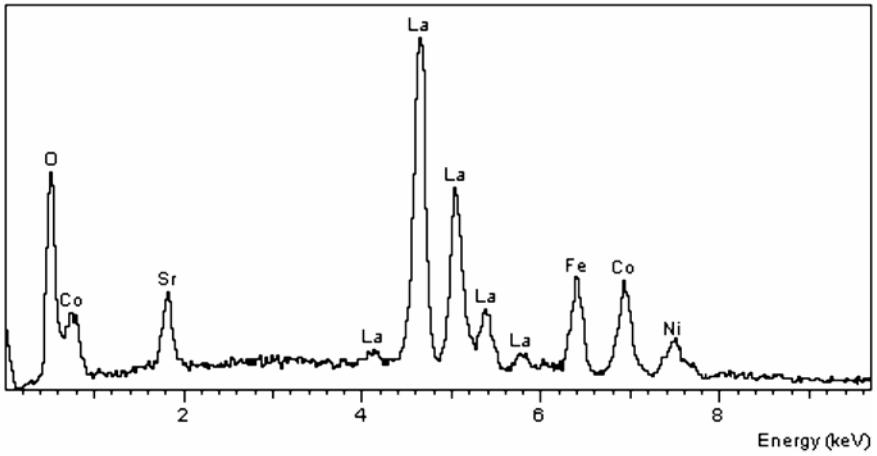

Fig. 2. Exemplary EDS spectrum of a $La_{0.8}Sr_{0.2}Co_{04}Fe_{0.4}Ni_{0.2}O_3$ sample

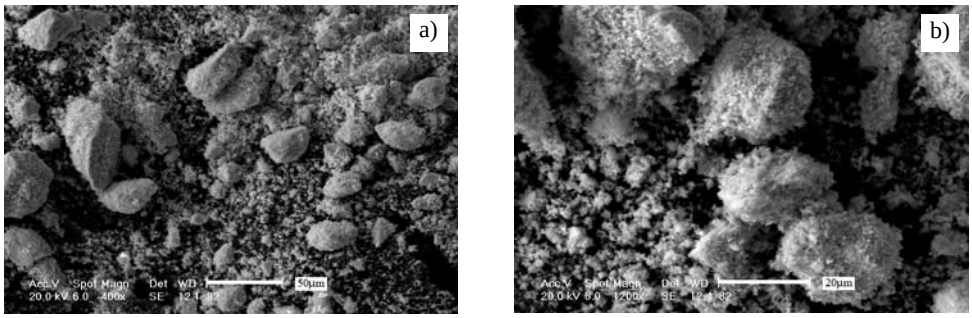

Fig. 3. SEM images of $La_{0.8}Sr_{0.2}Co_{0.4}Fe_{0.4}Ni_{0.2}O_3$ powder: a) 400×, b) 1200×

The exemplary EDS measurement of a $La_{0.8}Sr_{0.2}Co_{0.4}Fe_{0.4}Ni_{0.2}O_3$ sample presented in Figure 2 shows an even distribution of elements, with appropriate La/Sr and Co/Fe/Ni ratios. This confirms that the citric acid method is suitable for obtaining perovskites in the La–Sr–Co–Fe–Ni system. Traces of Cu, probably from nitrides and carbon, coming from the decomposition of citric acid, can also be detected. Scanning electron microscopy images of $La_{0.8}Sr_{0.2}Co_{0.4}Fe_{0.4}Ni_{0.2}O_3$ powder, presented in Figure 3, show rather a typical microstructure of the ceramic material obtained by heating

of the low temperature precursor. Agglomerates with sizes in the 5–50 μm range, consisting of < 1 μm crystallites, are observed. Similar microstructures were observed for other compositions.

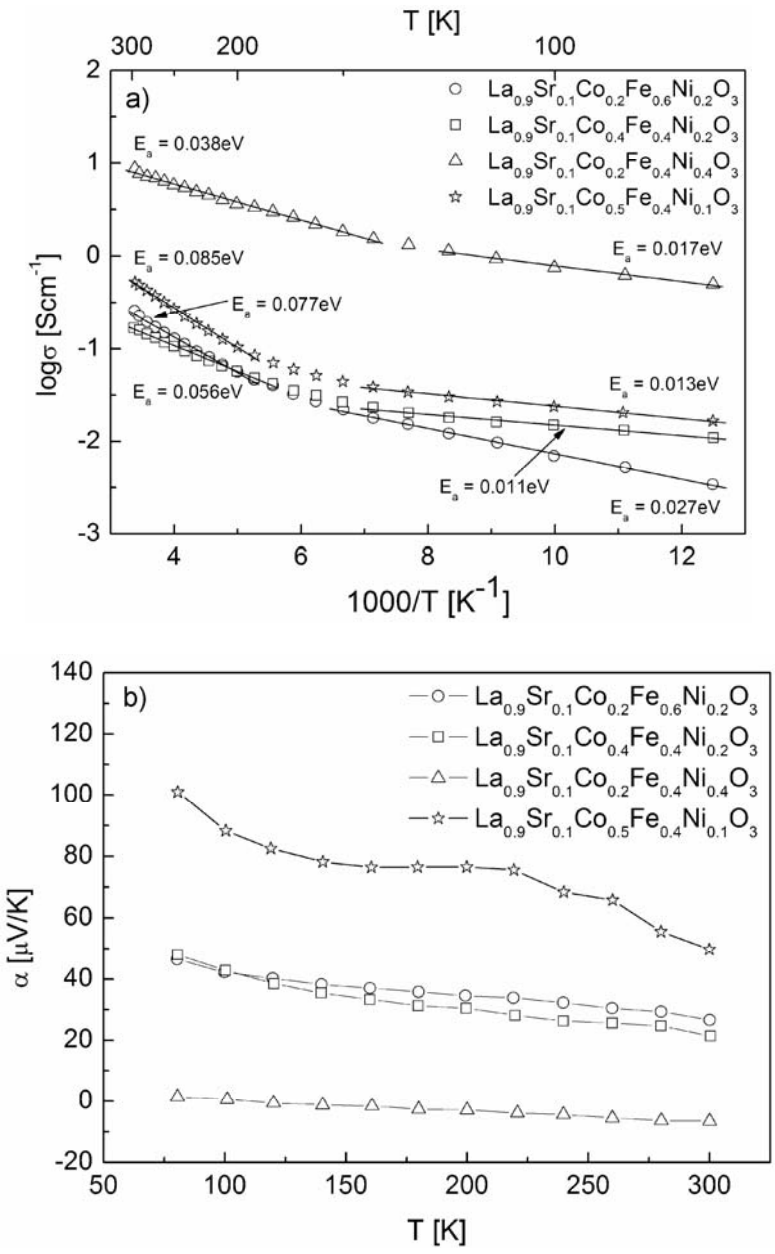

Fig. 4. Low-temperature (77–300 K) transport properties of $La_{0.9}Sr_{0.1}Co_{1-y-z}Fe_yNi_zO_3$ perovskites: a) electrical conductivity, b) thermoelectric power

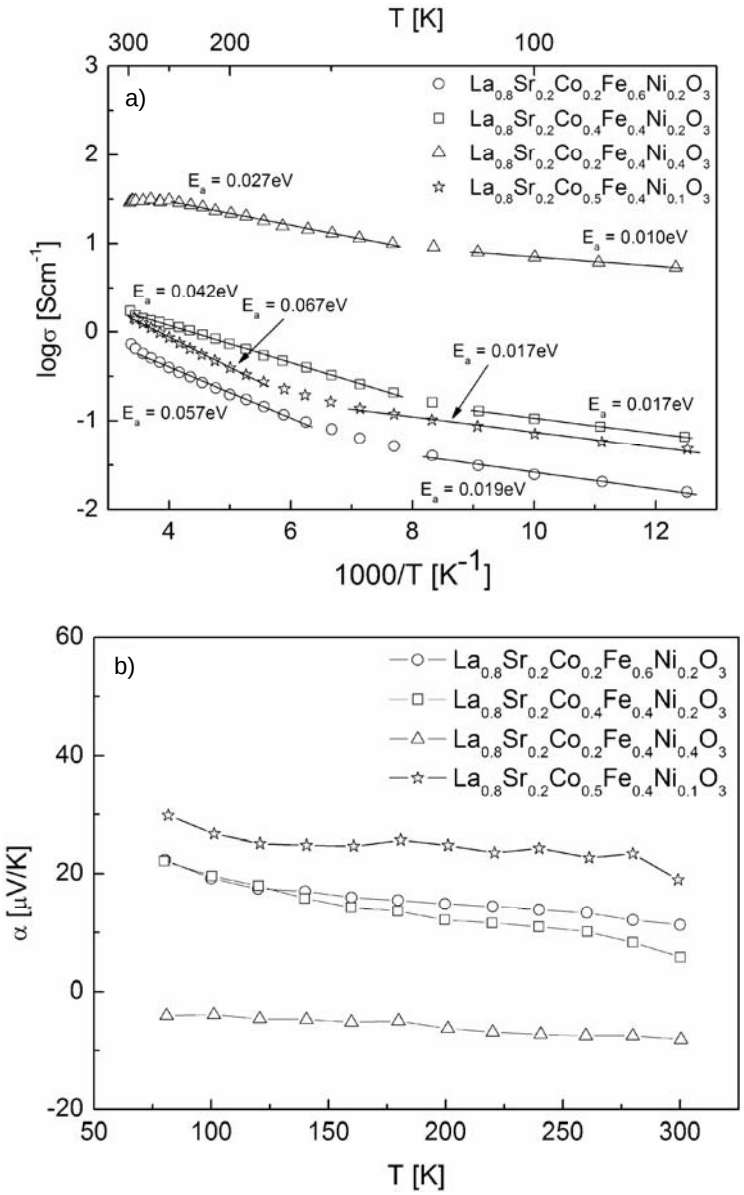

Fig. 5. Low-temperature (77–300 K) transport properties of $La_{0.8}Sr_{0.2}Co_{1-y-z}Fe_yNi_zO_3$ perovskites; a) electrical conductivity, b) thermoelectric power

The results of transport property measurements at low temperatures (77–300K) for $La_{0.9}Sr_{0.1}Co_{1-y-z}Fe_yNi_zO_3$ and $La_{0.8}Sr_{0.2}Co_{1-y-z}Fe_yNi_zO_3$ samples are presented in Figures 4 and 5. The observed dependence of electrical conductivity in a $\log\sigma$–$1/T$ plot cannot be fitted linearly in the entire temperature range. Two regions appear, one with a lower activation energy in the lower temperature range, and the other with a higher

activation energy in the higher temperature range. The highest electrical conductivity and low activation energies are observed for $La_{1-x}Sr_xCo_{0.2}Fe_{0.4}Ni_{0.4}O_3$ samples. This

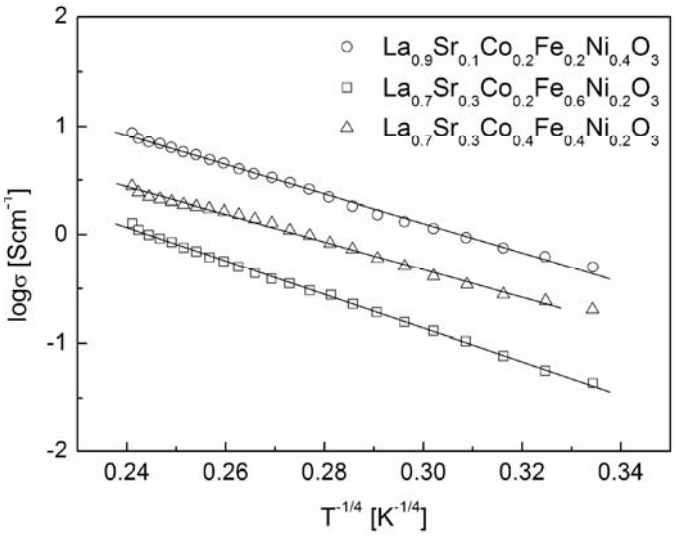

Fig. 6. Electrical conductivities of selected $La_{1-x}Sr_xCo_{1-y-z}Fe_yNi_zO_3$ perovskites in the low-temperature range (77–300 K), presented in a $\log\sigma - T^{-1/4}$ plot

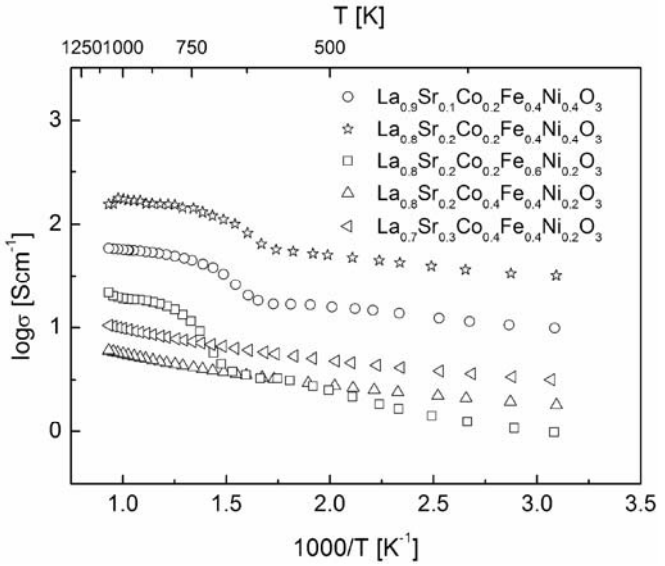

Fig. 7. Electrical conductivities of selected $La_{1-x}Sr_xCo_{1-y-z}Fe_yNi_zO_3$ perovskites at high temperatures

may be attributed to a higher Ni concentration, which leads to more metallic-like characteristics [7]. The influence of Co concentration on transport properties in the examined composition range is rather small. Similar effects can be observed in the

dependence of thermoelectric power on temperature. For $La_{1-x}Sr_xCo_{0.2}Fe_{0.4}Ni_{0.4}O_3$ samples, the thermoelectric power is negative in almost the entire temperature range, contrary to other samples. A negative TEP means that electrons are the dominant charge carriers. In Figure 6, the dependences of the electrical conductivity of selected $La_{1-x}Sr_xCo_{1-y-z}Fe_yNi_zO_{3-\delta}$ samples in a $\log\sigma$–$T^{-1/4}$ plot are presented. The observed linear dependence in these coordinates may be explained by using the 3D variable hopping range approach, which has also been observed in other perovskites [8].

High-temperature dc electrical conductivity measurements for selected $La_{1-x}Sr_xCo_{1-y-z}Fe_yNi_zO_3$ perovskites are presented in Figure 7. The change in the slope of the electrical conductivity, observed in the 600–750 K temperature range, can be related to a structural phase transition from hexagonal symmetry to a structure with higher symmetry. Relatively high electrical conductivity for samples with higher Sr and Ni content (175 $S\cdot cm^{-1}$ for $La_{0.8}Sr_{0.2}Co_{0.2}Fe_{0.4}Ni_{0.4}O_3$ at 1023 K) points to the necessity of further studies of perovskites from the (La, Sr)(Co, Fe, Ni)O_3 system.

4. Conclusions

The measured high-temperature (870–1070 K) dc electrical conductivity is relatively high for samples with high Sr and Ni content and needs further studies of perovskites belonging to the (La, Sr)(Co, Fe, Ni)O_3 system. The results of measurements suggest that optimised $La_{1-x}Sr_xCo_{1-y-z}Fe_yNi_zO_3$ samples in terms of chemical composition may possess attractive properties as cathode materials for IT–SOFCs.

Acknowledgements

This work is supported by the Polish Committee for Scientific Research under grant No. 3 T08A 013 26. One of the authors (K. Ś.) would like to thank the Foundation for Polish Science for financial support in the form of The Annual Stipends for Young Scientists program.

References

[1] SKINNER S.J., Fuel Cells Bull., 33 (2001), 6.
[2] IVERS-TIFFEE E., WEBER A., HERBSTRITT D., J. European Ceramic Soc., 21 (2001), 1805.
[3] CHIBA R., YOSHIMURA F., SAKURAI Y., Solid State Ionics, 124 (1999), 281.
[4] JIANG S.P., Solid State Ionics, 146 (2002), 1.
[5] KHARTON V.V., VISKUP A.P., BOCHKOV D.M., NAUMOVICH E.N., REUT O.P., Solid State Ionics, 110 (1998), 61.
[6] ŚWIERCZEK K., MARZEC J., OJCZYK W., MOLENDA J., Defect and Diffusion Forum, 237–240 (2005) 1293.
[7] CHAINANI A., SARMA D.D., DAS I., SAMPATHKUMARAN E.V., J. Phys.: Condens. Matter, 8 (1996), L631.
[8] JUNG W.-H., Physica B, 304 (2001), 75.

Received 10 December 2004
Revised 10 January 2005